ELSEVIER

Catalysis Today 52 (1999) 363–376

CATALYSIS TODAY

www.elsevier.com/locate/cattod

Examples of hydrogenation in semibatch and continuous slurry reactors

E. Santacesaria*, M. Di Serio, P. Iengo

Dipartimento di Chimica, dell'Università di Napoli Federico II, Via Mezzocannone 4, 80134 Napoli, Italy

Abstract

The present paper describes the problems arising in studying the kinetics of hydrogenation performed in slurry reactors and the ways to solve them. Two examples are considered: the hydrogenation of 2-ethyltetrahydroanthraquinone, an important step of the industrial production of hydrogen peroxide, and the partial hydrogenation of a rapeseed oil. Both hydrogenations were performed on the same palladium-supported catalyst.

Keywords: 2-Ethyltetrahydroanthraquinone; Rapeseed oil; Slurry reactors

1. Introduction

Many hydrogenation reactions of industrial interest are performed in either semibatch or continuous slurry reactors. In particular, we remember the examples of the hydrogenation of fatty oils and of 2-ethyltetrahydroanthraquinone, being this last a step of the industrial production of hydrogen peroxide. The collection and elaboration of kinetic data for these types of reaction can be difficult, because of: (i) the influence of mass transfer on reaction rates; (ii) the intervention of side reactions with the formation of by-products; (iii) the activation in situ of the catalyst with a delayed start of the reaction; (iv) the catalyst deactivation by poisoning. All these difficulties intervene in the two above examples and we will examine in this work how to perform the kinetic study. An attempt will be made to set out the problem in a general way starting from the observations collected in previously published experimental works [1–4] and in reviews and books devoted to slurry reactors [5–8].

The determination of the rate law for the mentioned examples requires a well-defined strategy in the experimental approach. Indeed, it is well known that reaction rates in slurry reactors can be affected not only by the liquid reactants concentration and by temperature, but also by the partial pressure of the gaseous reactant, the stirring rate and the catalyst hold-up. The simplest strategy usually adopted in programming kinetic runs is that of making experiments at low temperatures in well-stirred reactors and in the presence of a thin powdered catalyst. This procedure should allow to operate by neglecting mass transfer contribution, but in any case it does not avoid the possible complication of catalyst deactivation or of side reactions either consuming or not consuming the gaseous reactant. Moreover, sometimes it is not pos-

*Corresponding author. Tel.: +39-81-547-6544; fax: +39-81-552-7771

E-mail address: santacesaria@chemna.dichi.unina.it (E. Santacesaria)

0920-5861/99/$ – see front matter
PII: S0920-5861(99)00088-7

sible to lower temperature at the desired level, because the liquid phase becomes too viscous or causes solidification as in the case of fatty oils. Then, in the case of very active catalysts, mass transfer limitations can hardly be eliminated and the use of thin powdered catalysts could determine an enhancement of the gas–liquid mass transfer rates [9] in a way similar to that usually observed for very fast gas–liquid reactions [10–12]. Therefore, the simplest above mentioned strategy could bring to erroneous or incomplete conclusions.

The determination of the kinetic law and related parameters from reaction rate data affected by mass transfer limitation can be made indirectly only, as shown in this paper.

2. The choice of the most suitable reactor for the measurement of the reaction rate

Well-stirred reactors are largely preferred for laboratory kinetic studies with respect to bubble column ones, because their data are easier to interpret. In particular, semibatch reactors are more used than continuous ones because of their simple realization and use. On the other hand, the use of continuous reactors is sometimes necessary, for example, when together with the kinetics of the main reaction other slower processes must be studied such as catalyst deactivation or side reactions, or when the main reaction occurs so fast that reaction rates cannot easily be measured in transient experiments.

For what concerns the reaction rates measurement we distinguish two cases: the reaction is very fast and is completed in few minutes or is less fast and occurs in more than 30 min. In the first case, kinetic runs performed in semibatch reactors consist only in the measurement of the gaseous reactant consumption rates with a flowmeter, while, in the second case, there is also the opportunity of withdrawing and analysing small samples of the liquid phase at different times. In this last case, we have reaction rate data from two different sources and information about the occurrence of side reactions.

In the case of a fast reaction, a continuous reactor could be used, but other experimental difficulties arise because in these simple flowing reactors it is not easy to keep the catalyst hold-up and the liquid level constant. All these difficulties have been met with in the two examples mentioned in the previous section herein, that is, the hydrogenation of 2-ethyltetrahydroanthraquinone and of fatty oils. In the first case, the hydrogenation of anthraquinone at the oxygen atom, in the presence of a palladium-supported catalyst is a very fast reaction. Together with this useful reaction, we have a slow deactivation of the catalyst and side reactions reducing the concentration of anthraquinones which are active in the production of hydrogen peroxide [3]. We used a semibatch stirred reactor to study both the fast reaction, and separately, the slow side reactions, while we used a continuous stirred tank reactor to study the catalyst deactivation [2]. We solved the problem of keeping constant the catalyst hold-up by placing a screen of metallic wires at the bottom of the reactor, while the liquid level was taken roughly constant with the aid of an automatic control [2]. At last, all the kinetic equations obtained and the related parameters have been tested by simulating the behavior of industrial bubble column reactors in different operative conditions.

The hydrogenation of fatty oils, in the presence of palladium-supported catalyst [4], is a moderately fast reaction. We have studied it in a semibatch stirred reactor. In this case, we evaluated both the consumption rate of hydrogen and the evolution with time of reactants and products by analyzing the liquid samples withdrawn at different times of reaction. The difficulty, in this case, is that together with triene, diene and monoene hydrogenation, *cis–trans* isomerization of the double bonds occurs.

3. Evaluation of the kinetic law equation in the presence of mass transfer limitation from data of hydrogen consumption rate

3.1. Collecting and elaborating reaction rates

A three-phase reaction system can be represented by the reaction scheme:

$$A_{(gas)} + zB \rightarrow P \quad (1)$$

Some steps occur before A molecules can be converted to products on the active sites of the catalyst and the concentration profile of the gaseous species A can be depicted as in Fig. 1.

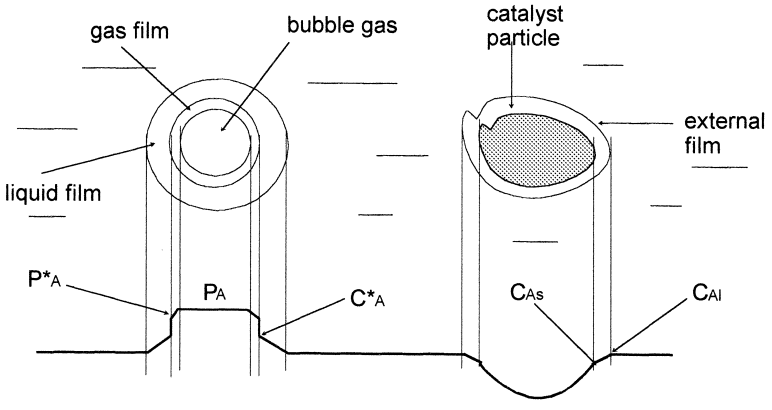

Fig. 1. Concentration profile of the gaseous A species through the different interfaces.

According to the classic approach [13], the following rate equations may be written for each diffusion step:

$$N_{g-g} = k_G a_L (P_A - P_A)$$

gas−liquid mass transfer rate (gas side) (2)

$$N_{g-l} = k_L a_L (C_A^* - C_{A_L})$$

gas−liquid mass transfer rate (liquid side) (3)

$$N_{l-s} = k_S a_S (C_{A_L} - C_{A_S})$$

liquid−solid mass transfer rate (4)

$$r = \eta f(m, C_A, C_B, T)$$

internal diffusion + reaction rate (5)

remembering that $a_S = 6m/(\rho_p d_p)$. For hydrogen, we can assume the validity of the Henry's law and hence $C_A^* = P_A/H_A$, by introducing the steady state assumption and the first order with respect to A for the kinetic equation, the relations can be equated; eliminating the interface concentrations we obtain

$$r = \frac{P_A}{H_A\left[1/k_G a_L + 1/k_L a_L + \left(\rho_p d_p/6k_s + 1/\eta k_1\right)1/m\right]} \quad (6)$$

If the reaction proceeds very slowly, we have the chemical regime and relation (6) becomes

$$r^\circ \simeq k_1 m P_A / H_A \quad (7)$$

For practical purposes the mass transfer limit is difficult to be seen at experimental level, because of the high catalyst loading required and it is better evaluated from the inverse reaction rate expression, by plotting $P_A/H_A r$ against $1/m$ (the reciprocal of the catalyst hold-up):

$$\frac{P_A}{H_A r} = \left(\frac{1}{k_G a_L} + \frac{1}{k_L a_L}\right) + \left(\frac{\rho_p d_p}{6k_S} + \frac{1}{\eta k_1}\right)\frac{1}{m} \quad (8)$$

considering the intercept and the slope of this plot, such as in Fig. 2 for the straight line.

If α, the reaction order of A is different from 1, trends of the plots $P_A/H_A r$ vs. $1/m$ are very different, as it can be appreciated still in Fig. 2. Therefore, by arranging reaction rates data obtained for different catalyst concentrations in plots such as that reported in Fig. 2, we can indirectly deduce information about the reaction order of the gaseous reactant that is fundamental for the successive step of calculating the effectiveness factor of the catalyst. As, in a semibatch reactor, the reaction rate can change during time, only the initial maximum rates are considered for drawing plots similar to those reported in Fig. 2, as in the example reported in Fig. 3.

However, it should be noted that there is no clear demarcation between chemical and mass transfer control and many runs such as that reported in Fig. 3 have, therefore, to be made by changing: catalyst hold-up, pressure of the gaseous reactant, concentration of the liquid phase reactant, temperature and stirring rate, in order to evaluate both the kinetic law, the related parameters and the influence of mass transfer in the employed reactor. The number of experiments required can greatly be reduced by performing the fluid-dynamic characterization of the reactor independently of the reaction.

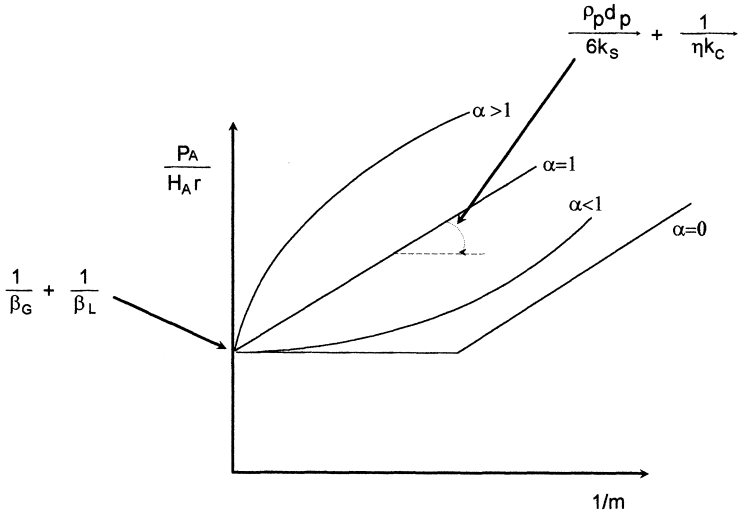

Fig. 2. Trends of $P_A/H_A r$ as a function of $1/m$ for different reaction orders α of the gaseous reagent.

3.2. *Fluid-dynamic characterization of a slurry reactor, determination of mass transfer parameters independently of the reaction*

Using pure hydrogen or well stirring the gas phase volume, the gas side gas–liquid mass transfer contribution can generally be neglected.

The product ($k_L a_L$) mainly depends on the fluid-dynamic characteristics of the reactor, that is, the shape, the size, the presence of baffles and mainly the type of turbine and the stirring speed. However, for a given reactor the stirring speed is the unique variable. It is useful, therefore, to define a reference mass transfer coefficient which is that obtained by measuring in transient experiments the rate of absorption or desorption of a gas, for example oxygen, in/from a well-stirred liquid but without forming any gas–liquid interphase area other than that easily measurable over the liquid. An amperometric electrode allows the determination of the evolution of the oxygen concentration during time. Data can be interpreted with the relation:

$$\pm\frac{dC_A}{dt} = k_L a_L\left(\frac{P_A}{H_A} - C_A\right) \tag{9}$$

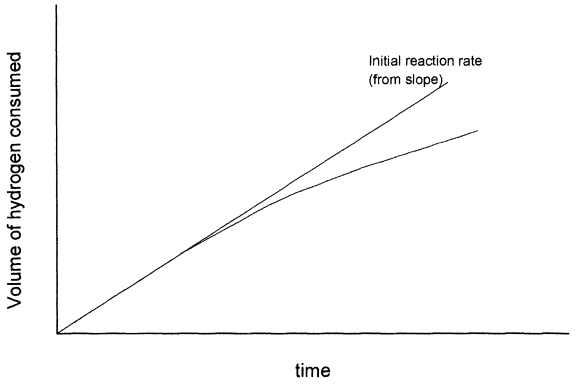

Fig. 3. Example of plot of the volume of hydrogen consumption during the time for kinetic run.

By integrating this relation after the introduction of the linear correlation existing between the oxygen concentration and the current intensity registered at the electrode, we obtain the simple relation [1]:

$$\frac{1}{a_L}\ln\left(\frac{1}{1 - i/i_{sat}}\right) = k_L t \tag{10}$$

So, we have a reference condition in which both the mass transfer coefficient and the interphase area are known. The effect of the rotating speed of the stirrer on the gas–liquid mass transfer rate starting from the reference condition can be determined by the well known sulfite method [14], that is by comparing the absorption rate of oxygen in a sodium sulfite aqueous

solution containing a salt of cobalt as catalyst, stirred at a given rotating speed, with that obtained in the reference condition. If the rotating speed is increased, both the gas–liquid interphase area and the mass transfer coefficient increase, consequently the product $\beta_L=k_La_L$ changes. It is fundamental for any reactor to have the trend of $\beta_L=k_La_L$ with the stirring speed.

It is then necessary to take account of the differences in the properties of the liquid solvents or of the gas used in the described experiments when performing the reaction to adjust the parameters with the aid, for example, of the Wilke and Chang relationship [15]. Semiempirical relations are also given in literature for the estimation of β_L in well-stirred reactors [5,6]. Obviously β_L can also be estimated or confirmed from the reaction rate data arranged in a plot such as that reported in Fig. 2. Reliable semiempirical relations exist also for the calculation of the liquid–solid mass transfer coefficients [5,6].

The values of a_S derive from the geometrical characteristics of the catalyst particles as it has been shown previously. Experimental evaluation of k_S can be made by considering, for example, the lowering rate of pH by reacting an alkaline aqueous solution with an acid exchange resin.

At last, internal diffusion can be treated in the classic way developed for gas–solid systems [13] but considering that diffusion coefficients in liquid phase are 1000–10 000 times lower than in gas phase; consequently, it is easy to show from the Thiele modulus relation:

$$\Phi = L\sqrt{\frac{kC_{AS}^{\alpha-1}}{D_{eff}}} \tag{11}$$

that in order to have the same value of the modulus for a reaction performed in the vapour or liquid phase, the size of the catalyst must be different by a factor of 30–100, that is, in a slurry reactor, we can have an effectiveness factor lower than 1 also for thin catalyst particles of 40–100 μm when chemical reactions are fast.

The solubility of the gaseous reactant appearing in many relationships in the form of the Henry's law constant must be known with good precision. Alternatively, it must be determined with independent experiments. In conclusion, only kinetic parameters must be determined by the regression analysis of the kinetic data.

4. Some minor effects influencing the hydrogenation rate and complicating the interpretation of the experimental kinetic data

Real feedstocks often contain catalyst poisons that quantitatively react with the catalyst. A certain amount of catalyst is necessary to neutralize the poison (threshold effect) and this amount must be neglected in the kinetic analysis [16].

In some cases an *induction effect* is operative, due to the formation in situ of the catalyst or to the catalyst protective coating removal. In these cases, after a defined *time-delay*, the observed rate constant approaches its full value k_r according to a first order function of the type [16]:

$$k = k_r(1 - e^{-wt}) \tag{12}$$

where w is the wash-out coefficient.

As it has been seen, when the reaction is very fast and the solution is poorly stirred, the concentration of the gaseous reactant can be zeroed in the liquid phase (*starvation effect*) and a small part of the catalyst is involved in promoting the reaction. When this catalyst is in the form of very thin particles and the reaction is very fast, the reaction occurs completely in the interfacial liquid film and the mass transfer rate is enhanced as it occurs in gas–liquid reactions [9]. However, the enhancement factors observed in slurry reactors are largely minor than those observed in gas–liquid reactors, not exceeding a value of 10–20 instead of 100–1000. This last aspect has not yet adequately been deepened in literature.

5. First example – hydrogenation of 2-ethylanthraquinone on a palladium-supported catalyst

The industrial production of hydrogen peroxide is mainly performed by subjecting a mixture of 2-ethylanthraquinone (EAQ) (30%) and 2-ethyltetrahydroanthraquinone (THEAQ) (70%) dissolved in a mixture of solvents to cyclic reductions and oxida-

tions, in the following scheme:

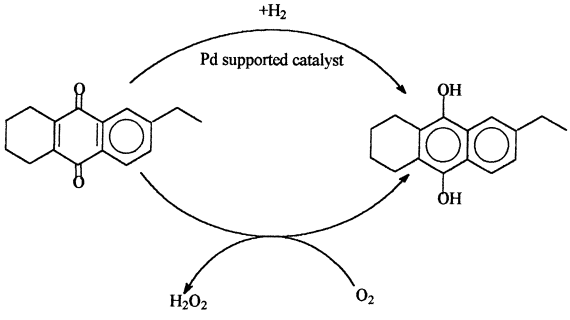

In the process named all-TETRA [17] only THEAQ is involved in the cycle of reaction because hydrogenation is usually kept at 70% conversion and the following equilibrium, completely shifted to the right, is operative [18]:

$$\mathrm{EAQ\ H_2 + THEAQ \leftrightarrow EAQ + THEAQ\ H_2} \qquad (13)$$

The hydrogenation step catalyzed by palladium-supported catalysts is a fast reaction occurring in few minutes in a semibatch reactor. Therefore, kinetic data are always affected by mass transfer limitations.

Kinetic runs can be performed only by measuring the rates of hydrogen consumption for different catalyst hold-up (catalyst employed: 2% by weight of palladium-supported on neutralized silica–alumina, with a surface area of the support 178 $m^2\ g^{-1}$ and of metal 149 $m^2\ g^{-1}$, density 0.77 g cm^{-3}, mean diameter of the particles 0.015 cm), different rpm of the stirrer, as well as different hydrogen pressure and substrate concentration. An example of the obtained trends of $(P_{H_2}/H_{H_2}r)$ against $1/m$ is reported in Fig. 4.

These trends suggest a zero order kinetic law for hydrogen, which can reasonably be justified by assuming first of all a dissociative chemisorption of hydrogen on the surface of palladium:

$$\mathrm{H_2} + 2\sigma \leftrightarrow 2\mathrm{H}\sigma \qquad (14)$$

The coverage degree of the surface will be, therefore

$$\theta_{H_2} = \frac{b_{H_2}C_{H_2}}{\left[1 + (b_{H_2}C_{H_2})^{1/2}\right]^2} \qquad (15)$$

Considering the strong affinity of hydrogen for palladium, we can also assume that $(b_{H_2}C_{H_2})^{1/2} \gg 1$. Then, all the kinetic runs can be well interpreted with an anthraquinone first order kinetic law, suggesting a Rideal–Eley mechanism of the type:

$$\mathrm{THEAQ} + 2\mathrm{H}\sigma \rightarrow \mathrm{THEAQH_2} + 2\sigma \qquad (16)$$

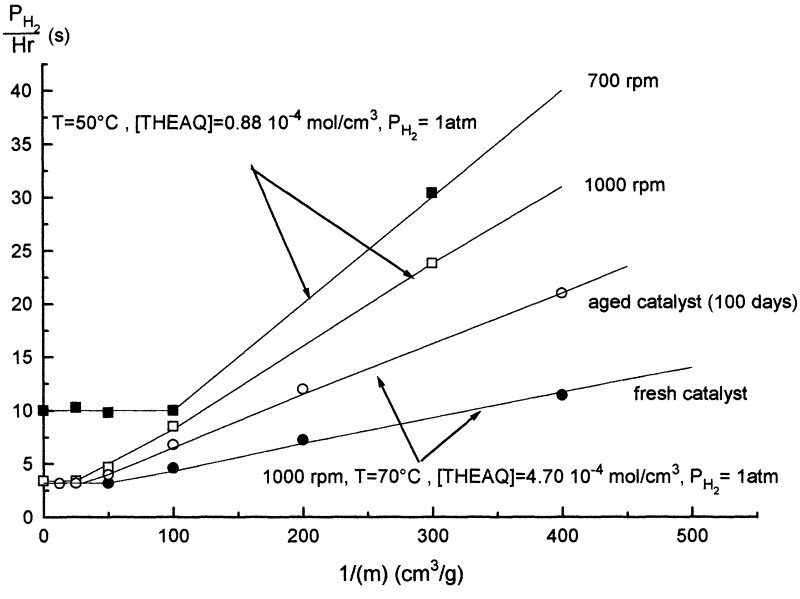

Fig. 4. Trends observed for P_{H_2}/Hr against $1/m$ for hydrogenation of THEAQ on palladium-supported catalyst in different conditions. Redraw from data reported in [2].

The kinetic law, derived from the experimental observations is

$$r = mk_1 C_{\mathrm{THEAQ}} \frac{b_{\mathrm{H_2}} C_{\mathrm{H_2}}}{\left[1 + (b_{\mathrm{H_2}} C_{\mathrm{H_2}})^{1/2}\right]^2} \approx mk_1 C_{\mathrm{THEAQ}} \tag{17}$$

In order to interpret kinetic runs, we must consider both mass transfer and reaction steps as seen above.

Ramachandran and Chaudari [5,6] defined the overall effectiveness factor as actual rate of reaction divided by the rate based on the inlet gas concentration and neglecting all the transport resistances, and described the way to calculate an overall effectiveness factor taking account of all the diffusional resistances for a zero order reaction. As the concentration of THEAQ is always much higher than that of hydrogen, we can consider this concentration constant along the time of an integration step, that is $k_1 C_{\mathrm{THEAQ}} = k_0$ (pseudo zero-order) and the value is then corrected before each successive integration step.

The overall effectiveness factor for a zero order reaction can be calculated according to Chaudari and Ramachandran [5,6] with the relation:

$$\eta^\circ = \eta_{\mathrm{D}} \left\{ 1 - \frac{\phi^{\circ 2}}{6} \left[1 - 3(1-\eta^\circ)^{2/3} + 2(1-\eta^\circ) \right] \right\} \tag{18}$$

where η_{D} is the overall effectiveness factor for a system completely dominated by external diffusion, that is

$$\eta_{\mathrm{D}} = \frac{P_{\mathrm{H_2}}}{H_{\mathrm{H_2}}} \frac{1}{(1/k_{\mathrm{L}}a_{\mathrm{L}} + 1/k_{\mathrm{S}}a_{\mathrm{S}}) mk^\circ} \tag{19}$$

For a very fast reaction η is negligible with respect to 1, consequently it results that $\eta \simeq \eta_{\mathrm{D}}$. Calculation starts with the evaluation of the ϕ° modulus:

$$\phi^\circ = R_{\mathrm{p}} \sqrt{\frac{k_0 \rho_{\mathrm{p}} H_{\mathrm{H_2}}}{D_{\mathrm{eff}} P_{\mathrm{H_2}}}} \tag{20}$$

Then, we calculate η_{D} and solve the η equation by finding the zero of the function:

$$F = \eta^\circ - \eta_{\mathrm{D}} \left\{ 1 - \frac{\phi^{\circ 2}}{6} \left[1 - 3(1-\eta^\circ)^{2/3} + 2(1-\eta^\circ) \right] \right\} \tag{21}$$

Now, the reaction rate can be determined as

$$r = \eta^\circ mk_0 \tag{22}$$

In order to make calculations, we need to know the following parameters: $\beta_{\mathrm{L}} = k_{\mathrm{L}}a_{\mathrm{L}}$, $\beta_{\mathrm{S}} = k_{\mathrm{S}}a_{\mathrm{S}}$, D_{eff}, $H_{\mathrm{H_2}}$ and their dependence on temperature. The kinetic constant k_0 can be determined by a mathematical regression analysis on the experimental runs. More details about the methods employed to determine the mentioned parameters for the hydrogenation of 2-ethyltetrahydroanthraquinone are reported in [2].

However, in the kinetic runs examined, η fallen in the range 0.02–0.15, that is, for this reaction, mass transfer limitations are always operative and reaction rates are strongly dependent on the adopted fluid dynamic conditions.

Together with hydrogenation at the oxygen of THEAQ, two other very slow processes occur: the deactivation of the catalyst and the hydrogenation at the aromatic rings of both EAQ and THEAQ. These phenomena can be neglected in the described kinetic study, but, on the contrary, need to be deepened for the relevant effects produced in industrial plants. Fig. 4 compares the plots of $P_{\mathrm{H_2}}/(H_{\mathrm{H_2}} r)$ vs. $1/m$ for a fresh and a 100 days aged catalyst, respectively, withdrawn from an industrial plant. Being the mean size of the particles nearly the same for the two catalysts, the difference observed in the slopes must be attributed to the difference in the kinetic constants as a consequence of poisoning. In order to study the kinetics of catalyst poisoning, a continuous reactor must be used operating for such a long time so to observe the decay of the catalytic activity. An example of such runs is reported in Fig. 5, where it can be observed that in correspondence of an increase of the water concentration a strong decrease of the catalyst activity occurs. When water concentration is kept constant, activities slowly decrease until reaching an equilibrium value.

We recognized that the poisoning effect observed can be attributed to the presence of small amounts of water in the solution; this effect is a reversible phenomenon. Water is generally dissolved to saturation in the anthraquinones solution and in these conditions causes the loss of about 30% of the catalytic activity in few days.

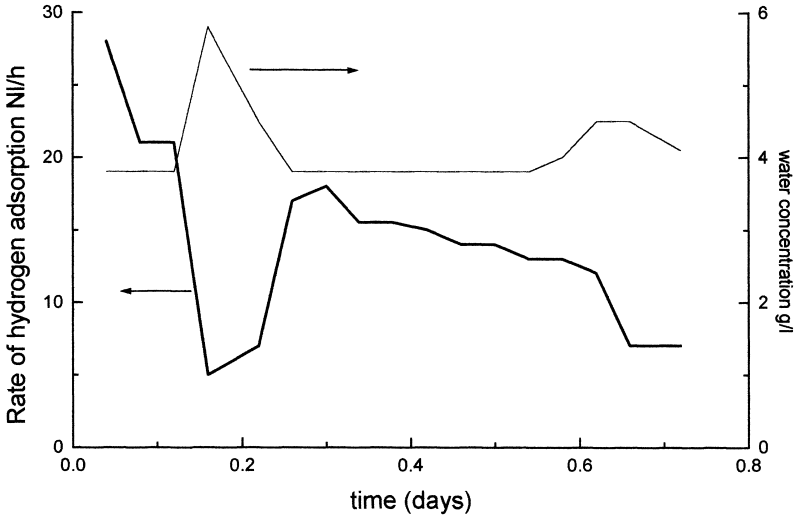

Fig. 5. The poisoning effect of water in the hydrogenation of THEAQ on palladium-supported catalyst. Redraw from data reported in [2].

The reversible poisoning should be due to the reaction:

$$2PdH + 2H_2O \rightleftharpoons 2Pd\text{----}O(H)(H) + H_2 \quad (23)$$

and as expected, it is affected by hydrogen pressure. By examining the industrial plant behavior, we discovered also the contribution of another much slower irreversible poisoning effect which is too slow to be studied in a laboratory reactor. We can put the kinetic constant of the hydrogenation reaction proportional to the fraction of the catalytic sites $\theta(t)$, i.e. $k=k_r\theta$. Initially $\theta=1$, while the evolution with time of θ, corresponding to the evolution of k, can be interpreted for the reversible poisoning with the relation:

$$\frac{d\theta}{dt} = -k'_d C_W \theta \left[1 - \frac{1}{K_{ed}} \frac{\theta_W P_{H_2}}{C_W \theta}\right] \quad (24)$$

Irreversible deactivation can be described by integrating the relation:

$$\frac{d\theta_0}{dt} = -k''_d \theta_0 \quad (25)$$

By integrating these two equations the evolution with time of the catalytic activity in an industrial plant operating for 30 days has been simulated using the parameters k'_d and K_{ed} determined by laboratory runs in the continuous reactor, while k''_d has been derived directly from the industrial reactor performances. It is interesting to observe that during the 30 days' industrial run, fresh catalyst must be added in order to keep the catalytic activity constant up to more than 40% of the initial amount. In Fig. 6 we can appreciate what happens to the activity simulation when catalyst poisoning is neglected.

The necessity to add fresh catalyst to keep constant the catalytic activity in the industrial reactor is the most relevant consequence of catalyst poisoning. Similarly, the occurrence of the slow process of hydrogenating the aromatic rings of EAQ or THEAQ has no consequence in the kinetic study performed in semibatch laboratory reactors of the oxygen hydrogenation, but cannot be neglected when simulating the behavior of a big sized continuous industrial plant, because of the loss of active quinones and the modification of the optimal ratio EAQ/THEAQ.

The necessity to add EAQ and to eliminate the accumulated products are consequence of these secondary reactions.

Finally, as EAQ is commercially available and THEAQ is not, the start-up of an industrial plant requires the production in situ of THEAQ by hydro-

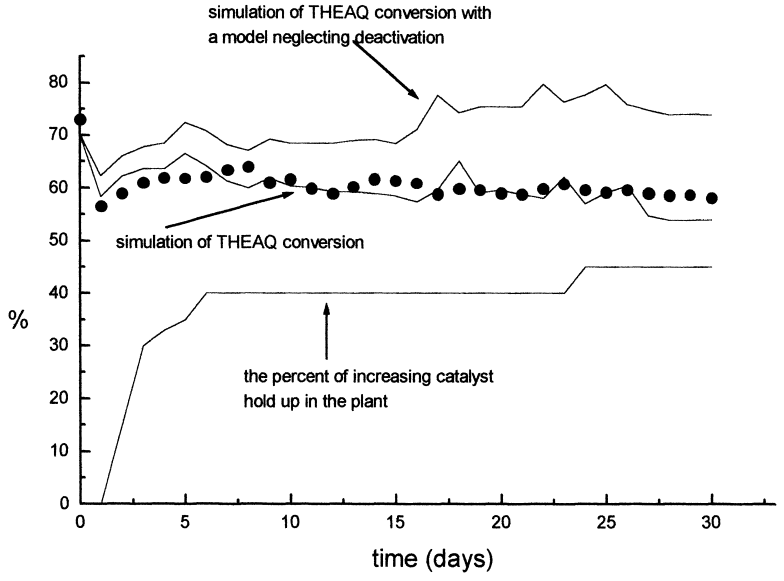

Fig. 6. Simulation of THEAQ hydrogenation in an industrial plant by considering or neglecting the poisoning effect.

genating one EAQ aromatic ring; stopping the reaction when the optimal EAQ/THEAQ ratio is reached. The reactions to be studied are

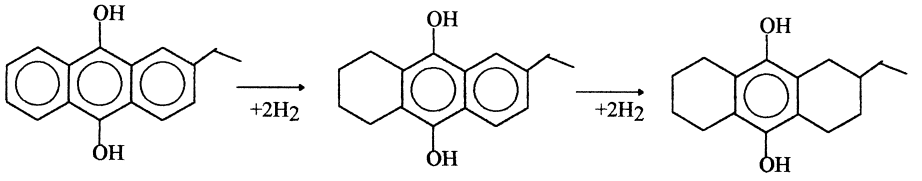

(EAQH2) (THEAQH2) (H8EAQH2) (26)

Also these products are not active to form hydrogen peroxide and lead to an accumulation in the working solution.

H_8EAQH_2 being an inactive quinone. Other secondary reactions occur such as, for example $EAQH_2$ tautomerization to oxanthrone, followed by the formation of anthrone and dianthrone [17]

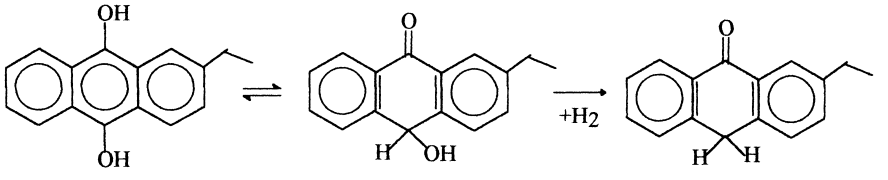

(27)

The kinetic study can easily be performed with long time runs in a semibatch laboratory reactor and by withdrawing and analyzing the reaction mixtures at different time in the classical way.

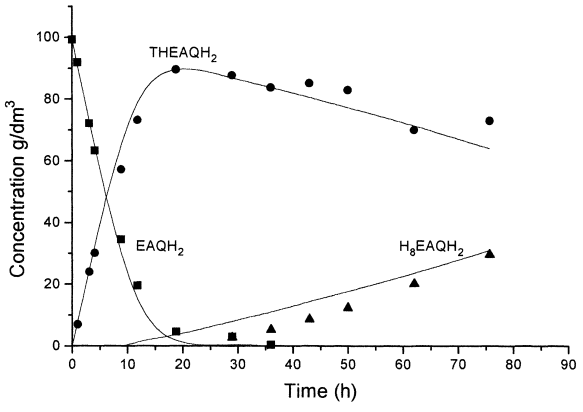

Fig. 7. Kinetic of EAQ aromatic rings hydrogenation. T=70°C, P=3 atm, m=0.013 g cm^{-3}. Redraw from data reported in [3].

The scheme of the reaction considered was

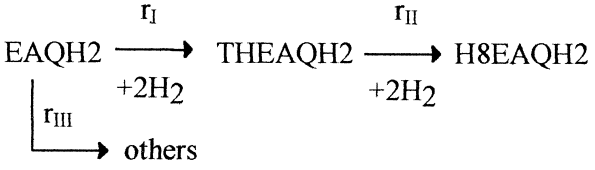

(28)

A first example of the kinetic runs performed is reported in Fig. 7. As it can be seen, the formation of H_8EAQH_2 is strongly prevented by the presence of EAQ. This behavior suggests a dual site mechanism for ring hydrogenation. Consequently, we assumed the following kinetic laws to simulate all the kinetic runs [3]:

$$r_I = \frac{mk_I b_{EAQH_2} C_{EAQH_2} P_{H_2}}{(1 + b_{EAQH_2} C_{EAQH_2} + b_{THEAQH_2} C_{THEAQH_2})^2} \quad (29)$$

$$r_{II} = \frac{mk_{II} b_{THEAQH_2} C_{THEAQH_2} P_{H_2}}{(1 + b_{EAQH_2} C_{EAQH_2} + b_{THEAQH_2} C_{THEAQH_2})^2} \quad (30)$$

$$r_{III} = mk_{III} C_{EAQH_2} \quad (31)$$

Tautomerization contributes to the loss of EAQ for about 5%.

Kinetic parameters determined by regression analysis of the experimental data are reported in [3,19].

6. Second example – hydrogenation of a rapeseed oil on a palladium-supported catalyst

The partial hydrogenation of a rapeseed oil in the presence of the same palladium-supported catalyst used in the previous example has been studied in the temperature range between 60°C and 120°C; we observed that diffusion limitations are always operative, in particular intraparticle ones. The kinetic approach is, therefore, the same as previously seen for the hydrogenation of 2-ethyltetrahydroanthraquinone. In spite of the masking effect of diffusion, a Langmuir–Hinshelwood kinetic law has been identified to well describe the behavior of the unsaturated molecules in the reaction, while the hydrogen reaction order has still been found to be equal to zero. In Fig. 8, an example of kinetic run is reported.

As it can be seen, hydrogenation of triene and diene occurs with similar rates while the hydrogenation of monoene seems to be prevented by the presence of polyunsaturated molecules.

Hydrogen consumption is reported in Fig. 9, for the same kinetic run as a function of time. The presence of an induction time can easily be recognized due to catalyst reduction.

By putting in a P_{H_2}/Hr plot the data of hydrogen consumption volume, a trend suggesting a zero order reaction for hydrogen is obtained. By considering the simple kinetic scheme:

$$T \underset{+H_2}{\overset{r_{idT}}{\rightarrow}} D \underset{+H_2}{\overset{r_{idD}}{\rightarrow}} M \underset{+H_2}{\overset{r_{idM}}{\rightarrow}} S \quad (32)$$

where T=trienic, D=dienic, M=monoenic and S=saturated fatty acid, and by assuming as rate determining step the superficial reaction, we can put

$$r_{idT} = \frac{\eta^\circ mk_{idT} b_T C_T}{1 + b_T C_T + b_D C_D + b_M C_M} \quad (33)$$

$$r_{idD} = \frac{\eta^\circ mk_{idD} b_D C_D}{1 + b_T C_T + b_D C_D + b_M C_M} \quad (34)$$

$$r_{idM} = \frac{\eta^\circ mk_{idM} b_M C_M}{1 + b_T C_T + b_D C_D + b_M C_M} \quad (35)$$

$$r^\circ = r_{idT} + r_{idD} + r_{idM} \quad (36)$$

We have assumed that hydrogen is not competing with the double bonds for an absorption site. This

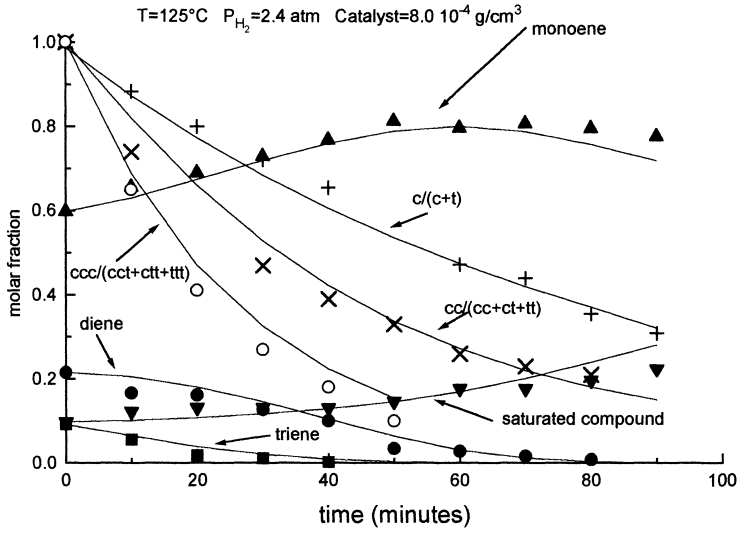

Fig. 8. An example of kinetic run for the hydrogenation of a rapeseed oil on a palladium-supported catalyst. Also the evolution with time of *cis/trans* isomerizations is reported. Redraw from data reported in [4].

assumption agrees with the reasonable mechanism according to which both atomic hydrogen and double bond should be adsorbed on the same metal atom before reacting. The theoretical kinetic approach is similar to that described in the first example and the reaction has been considered as pseudo zero-order reaction by putting

$$k_0 = \frac{k_{i\mathrm{dT}} b_{\mathrm{T}} C_{\mathrm{T}} + k_{i\mathrm{dD}} b_{\mathrm{D}} C_{\mathrm{D}} + k_{i\mathrm{dM}} b_{\mathrm{M}} C_{\mathrm{M}}}{1 + b_{\mathrm{T}} C_{\mathrm{T}} + b_{\mathrm{D}} C_{\mathrm{D}} + b_{\mathrm{M}} C_{\mathrm{M}}} \tag{37}$$

and adjusting it at any integration step to take account of the change in the concentration of the unsaturated

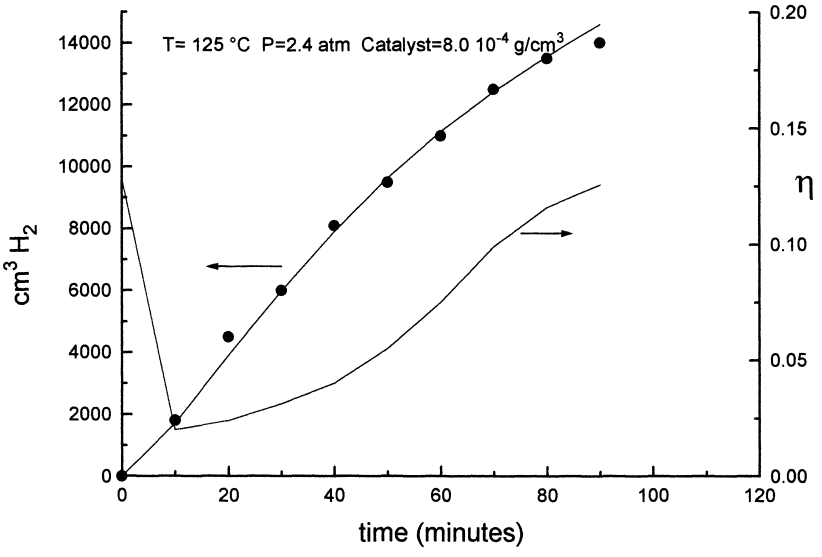

Fig. 9. Hydrogen consumption during the time for same kinetic run reported in Fig. 8. In this figure is also reported the evolution with time of the overall effectiveness factor. Redraw from data reported in [4].

compounds. The induction time was interpreted with the same kinetic model but using kinetic constants that were about five times lower. A 3/2/1 ratio between the adsorption constants of trienic, dienic and monoenic compounds was assumed roughly corresponding to the different probability of double bond interaction with the palladium surface. The kinetic parameters obtained by mathematical regression analysis of the experimental data have been reported [4].

Moreover, the kinetic model of fatty oil hydrogenation is much more complicated when considering also the occurring *cis–trans* isomerization reactions, not requiring hydrogen. A possible complete reaction scheme could be the following:

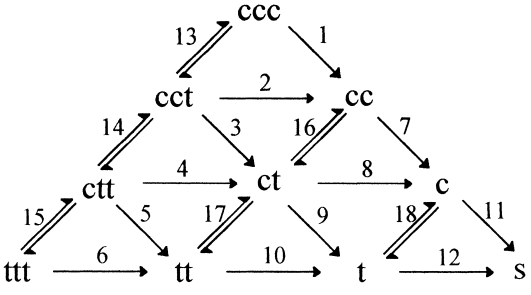

where *c* corresponds to a double bond with *cis* configuration and *t* the corresponding *trans* configuration, while *s* is the completely hydrogenated compound.

In the scheme, 12 hydrogenation and 6 *cis–trans* isomerization reactions are reported. We know the kinetic laws for the hydrogenation reactions, being the same previously seen, opportunely adapted, that is:

$$r_j = \frac{nm\eta^{\circ} k_{id\mathrm{T/D/M}} b_{\mathrm{T/D/M}} C_{\mathrm{SUB}_i}}{1 + b_{\mathrm{T}} C_{\mathrm{T}}^{\mathrm{t}} + b_{\mathrm{D}} C_{\mathrm{D}}^{\mathrm{t}} + b_{\mathrm{M}} C_{\mathrm{M}}^{\mathrm{t}}} \tag{38}$$

with j=1–12 while C_{SUB_i} corresponds to the concentration of one of the 9 hydrogenable molecules involved in the 12 reactions. n corresponds to the hydrogenation probability for a specific double bond in a polyunsaturated molecule and it can be 1, 1/3, 2/3, 1/2. $k_{id\mathrm{T/D/M}}$ is the hydrogenation kinetic constant, obviously different for molecules of triene ($k_{id\mathrm{T}}$), diene ($k_{id\mathrm{D}}$) and monoene ($k_{id\mathrm{M}}$). $b_{\mathrm{T/D/M}}$ is the adsorption term, that is, b_{T}, b_{D}, or b_{M} according to the involved molecule triene, diene or monoene. $C_{\mathrm{T}}^{\mathrm{t}}$, $C_{\mathrm{D}}^{\mathrm{t}}$ and $C_{\mathrm{M}}^{\mathrm{t}}$ are the overall concentrations of triene, diene and monoene, respectively, for example $C_{\mathrm{T}}^{\mathrm{t}} = C_{\mathrm{ccc}} + C_{\mathrm{cct}} + C_{\mathrm{ctt}} + C_{\mathrm{ttt}}$

By applying to the *cis–trans* isomerization reaction a reasonable Langmuir–Hinshelwood kinetic law and considering the reaction far from the equilibrium, it results:

$$r_h = \frac{mk_{i\mathrm{S}} b_{\mathrm{T/D/M}} C_{\mathrm{SUB_c}}}{1 + b_{\mathrm{T}} C_{\mathrm{T}}^{\mathrm{t}} + b_{\mathrm{D}} C_{\mathrm{D}}^{\mathrm{t}} + b_{\mathrm{M}} C_{\mathrm{M}}^{\mathrm{t}}} \tag{39}$$

where h=13–18 and $C_{\mathrm{SUB_c}}$ is the concentration of one of the isomerizable molecules and $C_{\mathrm{SUB_t}}$ that of concentration of the corresponding isomerized molecules.

The value of the isomerization kinetic constant obtained by regression analysis have also been reported in [4].

Rates r_{13} to r_{18} are slow if compared with those of hydrogenation and the effectiveness factors are generally equal to 1. The Langmuir–Hinshelwood kinetic model gives a satisfactory agreement with the experimental evolution of *cis* and *trans* species during the time as it can be seen in Fig. 8; though being questionable, this model helps in understanding the occurring reaction mechanisms and in rationally comparing the behavior of different catalysts.

7. Conclusions

We have seen that the kinetics of fast hydrogenation reactions such as THEAQ hydrogenation can be studied in semibatch laboratory reactors by interpreting the data of hydrogen consumption giving indirect information about the hydrogen reaction order. In the presence of palladium this order is often zero. The kinetics of less fast hydrogenation reactions, such as the hydrogenation of fatty oils, can be studied in the same way but in this case other information can be achieved from the analysis of the samples of the liquid reaction mixture taken at different times. Slow phenomena occurring together with the main hydrogenation reactions such as catalyst deactivation or by-products formation do not interfere with the kinetic study, but could have negative consequences in the large size continuous industrial reactors. Therefore, the kinetics of these slow phenomena must be studied independently, by means of long time runs performed as needed in semibatch or continuous reactors.

8. Nomenclature

a_L specific gas–liquid interface area (cm^{-1})
a_S specific liquid–solid interface area (cm^{-1})
b_i adsorption equilibrium constant of i species ($cm^3\ mol^{-1}$)
C_i^* reacting gas i concentration in equilibrium with P_i (mol cm^{-3})
C_i concentration of i in the liquid bulk (mol cm^{-3})
C_{i_S} reacting gas i concentration at the solid surface (mol cm^{-3})
D_{eff} effective diffusion coefficient ($cm^2\ s^{-1}$)
d_p average diameter of the catalyst particles (cm)
H_i Henry's parameter for the solubility of i ($cm^3\ mol^{-1} atm^{-1}$)
i actual measured current (A)
i_{sat} saturation measured current (A)
k_n rate costant of first n order ($cm^{3n}\ g^{-1}\ mol^{1-n}\ s^{-1}$)
k'_d rate constant of reversible catalyst poisoning ($cm^3\ mol^{-1}\ day^{-1}$)
k''_d rate constant of irreversible catalyst poisoning (day^{-1})
k_{idi} rate constant of hydrogenation of i species (mol g^{-1} s)
k_I rate constant of hydrogenation of aromatic ring of $EAQH_2$ (mol $g^{-1}\ atm^{-1}\ h^{-1}$)
k_{II} rate constant of hydrogenation of aromatic ring of $THEAQH_2$ (mol $g^{-1}\ atm^{-1}\ h^{-1}$)
k_{III} rate constant of $EAQH_2$ degradation ($cm^3\ g^{-1}\ h^{-1}$)
k_L gas–liquid mass transfer coefficient (cm s^{-1})
k_S liquid–solid mass transfer coefficient (cm s^{-1})
K_{ed} equilibrium constant for the reversible catalyst poisoning (atm mol cm^3)
L volume of catalyst particles/external surface (cm)
m catalyst hold-up (g cm^{-3})
P_i pressure of i (atm)
r° overall rate of oil hydrogenation
t time (s)
T temperature

Greek letter

α reaction order of gaseous reagent
η effectiveness factor related to the catalyst particles
η° overall effectiveness factor
ϕ Thiele parameter
ρ_p catalyst particle density (g cm^{-3})
θ_i fraction of catalyst sites occupied by i
θ_0 fraction of available sites, i.e., not permanently poisoned, initially equal to 1

Subscript

W water
T Triene
D Diene
M Monoene

Acknowledgements

Thanks are due to Ausimont SpA and Novamont SpA for the financial support.

References

[1] E. Santacesaria, P. Wilkinson, P. Babini, S. Carrà, Ind. Eng. Chem. Res. 27(5) (1988) 780.
[2] E. Santacesaria, M. Di Serio, R. Velotti, U. Leone, Ind. Eng. Chem. Res. 33(2) (1994) 277.
[3] E. Santacesaria, M. Di Serio, R. Velotti, U. Leone, J. Mol. Catal. 94 (1994) 37.
[4] E. Santacesaria, P. Parrella, M. Di Serio, G. Borrelli, Appl. Catal. 116 (1994) 269.
[5] R.V. Chaudari, P.A. Ramachandran, AIChE J. 26(2) (1980) 177.
[6] P.A. Ramachandran, R.V. Chaudari, Three-Phase Catalytic Reactors, Gordon and Breach, London, 1983.
[7] Y.T. Shah, Gas-Liquid-Solid reactors design, McGraw-Hill, New York, 1979.
[8] R.V. Chaudari, Y.T. Shah, N.R. Foster, Catal. Rev.-Sci. Eng. 28(4) (1986) 431.
[9] E. Alper, B. Wichtendahl, W.D. Deckwer, Chem. Eng. Sci. 35 (1980) 217.
[10] J.C. Charpentier, Mass Transfer Rate in Gas-Liquid Adsorber and Reactors, Advances in Chemical Engineering, Academic Press, New York, 1981.
[11] P.V. Danckwerts, Gas Liquid Reactions, McGraw-Hill, New York, 1970.
[12] G. Astarita, Mass Transfer with Chemical Reaction, Elsevier, Amsterdam, 1967.

[13] C.N. Satterfield, T.K. Sherwood, The Role of Diffusion in Catalysis, Addison-Wesley, New York, 1963.
[14] V. Link, V. Vacek, Chem. Eng. Sci. 36 (1981) 1747.
[15] C.R. Wilke, P. Chang, AIChE J. 1 (1955) 264.
[16] W.R. Alcorn, T.J. Sullivan, in: J.R. Kosak (Ed.), Catalysis of Organic Reactions, Marcel Dekker, New York, 1981.
[17] T. Ulmann, Encyclopedia of Industrial Chemistry, vol. A13, VCH, Weinheim, 1989, p. 443.
[18] T. Berglin, N.H. Shöön, Ind. Eng. Chem. Process Des. Dev. 22 (1983) 150.
[19] E. Santacesaria, M. Di Serio, R. Velotti, U. Leone, J. Mol. Catal. 99 (1995) 151.